ECCOMAS Congress 2016
VII European Congress on Computational Methods in Applied Sciences and Engineering
M. Papadrakakis, V. Papadopoulos, G. Stefanou, V. Plevris (eds.)
Crete Island, Greece, 5–10 June 2016

TOPOLOGY OPTIMIZATION OF WAVE BARRIERS FOR RAILWAY INDUCED VIBRATIONS IN BUILDINGS

Cédric Van hoorickx[1], Mattias Schevenels[2], and Geert Lombaert[1]

[1]KU Leuven, Department of Civil Engineering, Structural Mechanics Section
Kasteelpark Arenberg 40, 3001 Leuven, Belgium
e-mail: {cedric.vanhoorickx,geert.lombaert}@bwk.kuleuven.be

[2] KU Leuven, Department of Architecture, Architectural Engineering
Kasteelpark Arenberg 1, 3001 Leuven, Belgium
e-mail: mattias.schevenels@asro.kuleuven.be

Keywords: Topology optimization, Railway induced vibration, Elastodynamic wave propagation, Wave barriers.

Abstract. *In order to reduce environmental ground vibration due to railway traffic, mitigation measures at the source, the transmission path and the receiver can be applied. Mitigation measures on the transmission path are particularly appealing in situations with existing track and buildings. In this contribution, the optimal design of stiff wave barriers is considered.*

Up to now, wall barriers with a rectangular cross section have mostly been studied. However, current construction methods of wave barriers provide a wide flexibility in design geometry. Therefore further improvement is feasible. Topology optimization is used to discover novel, improved design geometries.

Stiffer material is inserted into a design domain located between the source and a building. The objective is to minimize the amount of stiffer material in the design domain while satisfying the required vibration criteria in the building. The optimization problem is solved using a gradient based method and the adjoint method is used to enable an efficient calculation of the sensitivities.

In this way, an optimal geometry is determined that considerably reduces the required amount of stiffer material. Topology optimized stiff wave barriers are therefore effective in reducing vibration levels, outperforming the rectangular wave barriers. The design contains, however, small features, making it sensitive to geometric imperfections, and a worst case robust optimization is applied. The resulting smaller sensitivity with respect to geometric imperfections also ensures that a posteriori design simplifications have a minimal impact on the barriers performance.

1 INTRODUCTION

Railway induced vibrations may lead to the malfunctioning of sensitive equipment, discomfort and structural damage at high vibration levels. Furthermore, noise can be re-radiated from floors and walls. This paper focuses on malfunctioning of sensitive equipment. Extensive research is performed to search for effective vibration mitigation measures. Three categories of mitigation measures are distinguished, namely at the source [1], the transmission path [2, 3] and the receiver [4]. These refer respectively to the railway track, the soil and the building. The present work considers wave barriers to hinder ground vibration propagation from source to receiver.

Currently, only a limited number of simple design geometries for mitigation measures have been investigated. However, current flexibility in construction methods, such as jet grouting, provides opportunities for further improvement. To discover novel design geometries, topology optimization is applied. Topology optimization, originally developed for static mechanical problems, is used for a variety of applications, including problems governed by wave propagation [5]. Examples include electromagnetic, elastomagnetic and acoustic applications, such as photonic crystal waveguide designs [6], designs of phononic band-gap materials [7] and noise barriers [8].

This study uses topology optimization to design barriers impeding elastodynamic wave transmission. Wave barrier effectiveness is quantified by comparing the calculated one-third octave band velocity spectra in specific receiver points in the building to generic vibration criteria for sensitive equipment [9]. Since full control of the built geometry is difficult in the construction of underground structures, the optimized design should be robust with respect to geometrical imperfections [10]. A worst case approach is applied to improve the robustness of the design [11, 12]. The resulting designs can be used to realize simplified design solutions, which are suited for construction and are robust with respect to geometric imperfections.

The paper starts with the introduction of the optimization problem and a brief review of the topology optimization approach. Next, results for optimized wave barriers are discussed. Finally, the sensitivity to geometric imperfections is analyzed and a simplified design is presented.

2 PROBLEM DESCRIPTION AND METHODOLOGY

2.1 Problem description

The considered problem is shown in figure 1 and consists of a building located at the surface of a homogeneous elastic halfspace, representing the soil. The soil (subscript '1', as abbreviation for material 1) has a mass density ρ_1 of $2000\,\mathrm{kg/m^3}$, a longitudinal wave velocity C_{p1} of $400\,\mathrm{m/s}$, and a shear wave velocity C_{s1} of $200\,\mathrm{m/s}$. The building (subscript 'bu') is a four-storey frame consisting of four floors and two spans, with a total width w_{bu} of $12\,\mathrm{m}$ and a total height h_{bu} of $12\,\mathrm{m}$. The thickness of the walls $t_{\mathrm{bu,w}}$ is equal to $0.25\,\mathrm{m}$, while the thickness of the slabs $t_{\mathrm{bu,s}}$ is equal to $0.20\,\mathrm{m}$. The walls and slabs are made of reinforced concrete with a mass density ρ_{bu} of $2500\,\mathrm{kg/m^3}$, a Young's modulus E_{bu} of $30\,\mathrm{GPa}$, and a Poisson's ratio ν_{bu} of 0.25.

The halfspace is excited at the surface by a vertical load at a distance of $25\,\mathrm{m}$ from the building. A line load with a uniform spectrum in the frequency range between $4\,\mathrm{Hz}$ and $8\,\mathrm{Hz}$ is applied. The problem can be modeled as a two-dimensional problem and is shown in figure 2. The aim is to reduce the vibration levels at specific receiver points in the building, in this case on the first floor in the span closest to the source. A horizontal receiver is considered in the middle of the floor, while two vertical receivers are considered at one fourth and in the middle

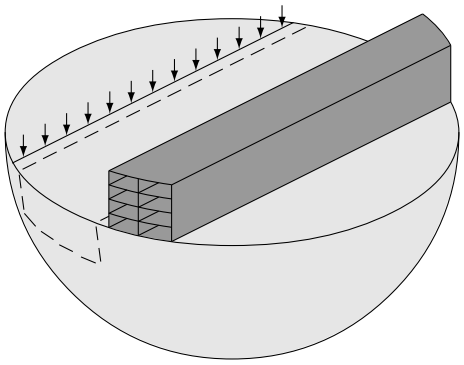

Figure 1: Semi-infinite halfspace excited at the surface close to a building.

of the floor span.

To reduce the vibration levels in these receiver points, a design domain with dimensions $8 \times 20\,\mathrm{m}^2$ is considered in the elastic halfspace, located between the source and the building. In this design domain a second stiffer material is introduced. This material (subscript '2') has a mass density ρ_2 of $2000\,\mathrm{kg/m}^3$, a longitudinal wave velocity $C_{\mathrm{p}2}$ of $950\,\mathrm{m/s}$, and a shear wave velocity $C_{\mathrm{s}2}$ of $550\,\mathrm{m/s}$.

The elastodynamic problem is solved using the finite element method with two-dimensional four-node elements in plane strain. For the mesh, an element size of $0.25\,\mathrm{m}$ is used, corresponding to ten elements per shear wavelength $\lambda_{\mathrm{s}1}$ at a frequency of 80Hz, the upper limit considered in this paper. In the design domain, however, the mesh size is reduced to $0.125\,\mathrm{m}$ to achieve a design with sufficient detail. The building is modeled using beam elements adapted to plane strain with an element size of $0.25\,\mathrm{m}$. The finite element equilibrium equations are written as:

$$\hat{\mathbf{K}}\hat{\mathbf{u}} = \hat{\mathbf{p}} \tag{1}$$

where $\hat{\mathbf{p}}$ is the load vector, $\hat{\mathbf{u}}$ is the displacement vector, and $\hat{\mathbf{K}}$ is the dynamic stiffness matrix, which depends on the frequency ω. At the boundaries of the finite element mesh, appropriate radiation boundary conditions have to prevent spurious wave reflections. The Perfectly Matched Layers (PML) of Harari and Albocher [13] are applied.

The one-third octave band velocity spectra are computed from the velocity spectra in the frequency domain:

$$\hat{v}_{m,i}^{\mathrm{RMS}} = \sqrt{\frac{1}{N_{\mathrm{f}}} \sum_{n=1}^{N_{\mathrm{f}}} \left|\hat{v}_{m,n,i}\right|^2} \tag{2}$$

where N_{f} is the number of frequencies in the one-third octave band with index m and i is the position of the receiver. This can be expressed as follows (since $\hat{v}_{m,n,i} = \mathrm{i}\omega\hat{u}_{m,n,i}$ with i the imaginary unit):

$$\hat{v}_{m,i}^{\mathrm{RMS}} = \sqrt{\frac{1}{N_{\mathrm{f}}} \sum_{n=1}^{N_{\mathrm{f}}} \omega_{m,n}^2 \left|\hat{u}_{m,n,i}\right|^2} = \sqrt{\frac{1}{N_{\mathrm{f}}} \sum_{n=1}^{N_{\mathrm{f}}} \omega_{m,n}^2 \hat{\mathbf{u}}_{m,n}^H \mathbf{L}_i \hat{\mathbf{u}}_{m,n}} \tag{3}$$

where $\mathbf{L}_i$ is a sparse selection matrix, equal to one at the diagonal element corresponding to the degree of freedom of receiver i.

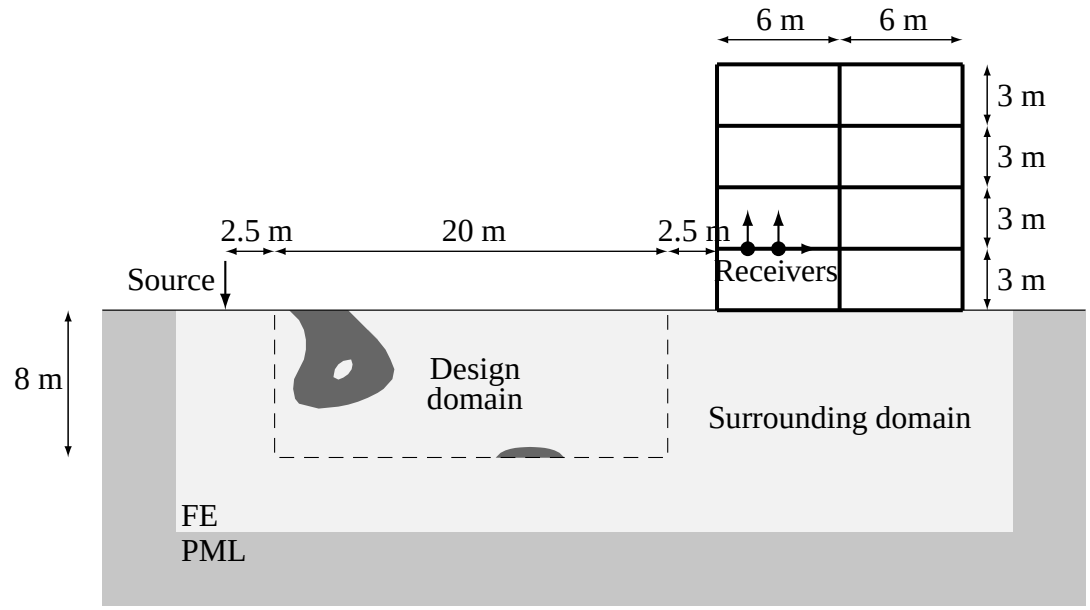

Figure 2: The two-dimensional optimization problem.

2.2 Topology optimization

Topology optimization [5] is used to optimally distribute the stiffer material in the design domain. The material distribution is parameterized using element densities $\bar{\rho}_e$ for each element e in the design domain. The value $\bar{\rho}_e = 0$ corresponds to the properties of the homogeneous halfspace, while the value $\bar{\rho}_e = 1$ corresponds to the properties of the stiffer material. Using a continuous interpolation of the densities between 0 and 1 makes it possible to solve the optimization problem with a gradient based method.

A Solid Isotropic Material with Penalization (SIMP) interpolation [14, 15] is used to interpolate the material properties α:

$$\alpha = \alpha_1 + \bar{\rho}_e^p \left(\alpha_2 - \alpha_1\right) \tag{4}$$

where α_1 and α_2 are the properties of the original and stiffer material, respectively. The penalization factor $p \geq 1$ avoids so-called gray designs with intermediate densities. A value $p = 1$ is used for the mass density ρ while $p = 3$ is used for the constrained modulus ρC_{p}^2 and the shear modulus ρC_{s}^2.

The (physical) element densities $\bar{\rho}_e$ are obtained from the design variables ρ_e of the optimization problem by applying a projection filter [16]:

$$\bar{\rho}_e = \frac{\tanh\left(\beta\eta\right) + \tanh\left(\beta(\tilde{\rho}_e - \eta)\right)}{\tanh\left(\beta\eta\right) + \tanh\left(\beta(1 - \eta)\right)} \tag{5}$$

with β a sharpness parameter, controlling the smoothness of the projection, η the projection threshold, and $\tilde{\rho}_e$ the intermediate densities obtained from:

$$\tilde{\rho}_e = \frac{\sum_{i=1}^{N} w_{ei} v_i \rho_i}{\sum_{i=1}^{N} w_{ei} v_i} \tag{6}$$

where v_i is the volume of element i and the weight $w_{ei} = \max(R - r_{ei})$ depends on the filter radius R and the center-to-center distance r_{ei} between the elements e and i. In the present work, the filter radius is taken to be $R = 6$ elements or $1.5\,\mathrm{m}$, the projection threshold value is set to $\eta = 0.5$ and the sharpness parameter β has an initial value equal to 1 and is continuously increased (multiplied by a factor 1.0116)such that the value of 32 is reached after 300 iterations.

2.3 Optimization problem

To quantify the effectiveness of the wave barriers, the calculated one-third octave band velocity spectra are compared with generic vibration criteria (VC) for sensitive equipment [9]. These criteria are specified in terms of the maximum allowable RMS velocity in the one-third octave bands between 4 and 80 Hz, as shown in figure 3a. The VC criteria impose less stringent vibration limits in the frequency range between 4 to 8 Hz, where the limit is that of constant acceleration instead of constant velocity.

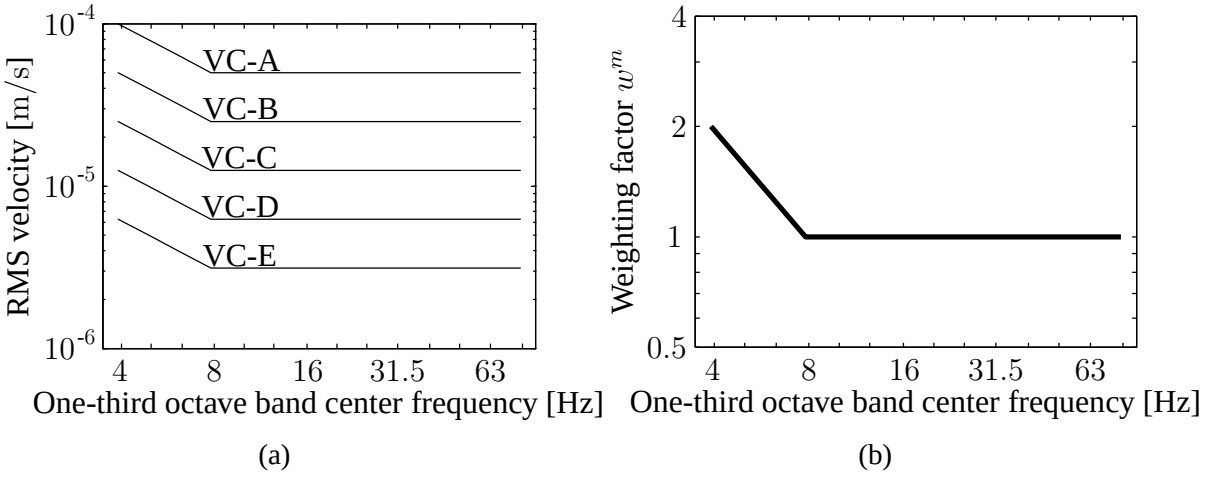

Figure 3: (a) Gordon's generic vibration criteria for sensitive equipment [9] and (b) the weighting function w_m proportional to the VC curves.

The aim is to reduce the vibration levels to meet the intended vibration criteria. However, since there is a cost in the amount of material that is stiffened, the volume of the wave barrier is minimized. The problem is reformulated as a minimization problem, where the volume is minimized and constraints are set on the vibration levels:

$$\begin{aligned} \min_{\rho_e} \quad & \sum_{e=1}^{N} v_e \bar{\rho}_e \\ \text{s. t.} \quad & \hat{v}_{m,i}^{\mathrm{RMS}}(\bar{\rho}_e) \leq w_m s, \quad m = 1 \cdots N_{\mathrm{band}} \\ & \qquad\qquad\qquad\quad\; i = 1 \cdots N_L \\ & 0 \leq \rho_e \leq 1, \qquad\quad e = 1 \cdots N_e \end{aligned} \tag{7}$$

with N_{band} the number of one-third octave bands considered, N_L the number of receiver points and N_e the number of elements in the design domain. The value s is the maximum allowable RMS velocity in the one-third octave bands between $8\,\mathrm{Hz}$ and $80\,\mathrm{Hz}$, for example equal to $12.5\,\mu\mathrm{m/s}$ for VC-C. The function w_m provides a correction for the one-third octave bands between $4\,\mathrm{Hz}$ and $8\,\mathrm{Hz}$, as is shown in figure 3b.

The optimization problem is solved using the method of moving asymptotes (MMA) [17]. Since this method is gradient-based, the derivatives of the objective function have to be calculated. The sensitivities are calculated using the chain rule:

$$\frac{\partial v_{m,i}^{\mathrm{RMS}}}{\partial \bar{\rho}_e} = \frac{1}{2N_{\mathrm{f}} v_{m,i}^{\mathrm{RMS}}} \sum_{n=1}^{N_{\mathrm{f}}} \omega_{m,n}^2 \frac{\partial \left[\hat{\mathbf{u}}_{m,n}^H \mathbf{L}_i \hat{\mathbf{u}}_{m,n}\right]}{\partial \bar{\rho}_e} \tag{8}$$

To efficiently calculate the derivative of the squared displacement modulus $\hat{\mathbf{u}}_{m,n}^H \mathbf{L}_i \hat{\mathbf{u}}_{m,n}$ to the physical densities $\bar{\rho}_e$, the adjoint method is used (see [5, p. 17]), resulting in:

$$\frac{\partial \left[\hat{\mathbf{u}}_{m,n}^H \mathbf{L}_i \hat{\mathbf{u}}_{m,n}\right]}{\partial \bar{\rho}_e} = 2\,\mathrm{Re}\left\{ \boldsymbol{\lambda}_{m,n,i}^T \frac{\partial \hat{\mathbf{K}}_{m,n}}{\partial \bar{\rho}_e} \hat{\mathbf{u}}_{m,n} \right\} \tag{9}$$

where the vector $\boldsymbol{\lambda}_{m,n,i}$ is computed from the adjoint equation, which can be written in the following simplified form:

$$\hat{\mathbf{K}}_{m,n} \boldsymbol{\lambda}_{m,n,i} = -\left(\frac{\partial \left[\hat{\mathbf{u}}_{m,n}^H \mathbf{L}_i \hat{\mathbf{u}}_{m,n}\right]}{\partial \hat{\mathbf{u}}_{m,n}} \right)^T = -\mathbf{L}_i \hat{\mathbf{u}}_{m,n}^* \tag{10}$$

3 OPTIMIZATION RESULTS

To show the effectiveness of a rectangular wave barrier, the influence of its thickness is analyzed. The rectangular wave barrier has a depth of $8\,\mathrm{m}$ and is located in the design domain as close as possible to the source, implying that the left boundary of the wave barrier is at a distance of $2.5\,\mathrm{m}$ from the source as follows from figure 2. The thickness is varied from $0\,\mathrm{m}$ to $20\,\mathrm{m}$, corresponding to the homogeneous halfspace and a fully filled design domain, respectively. This is done in steps of $0.5\,\mathrm{m}$.

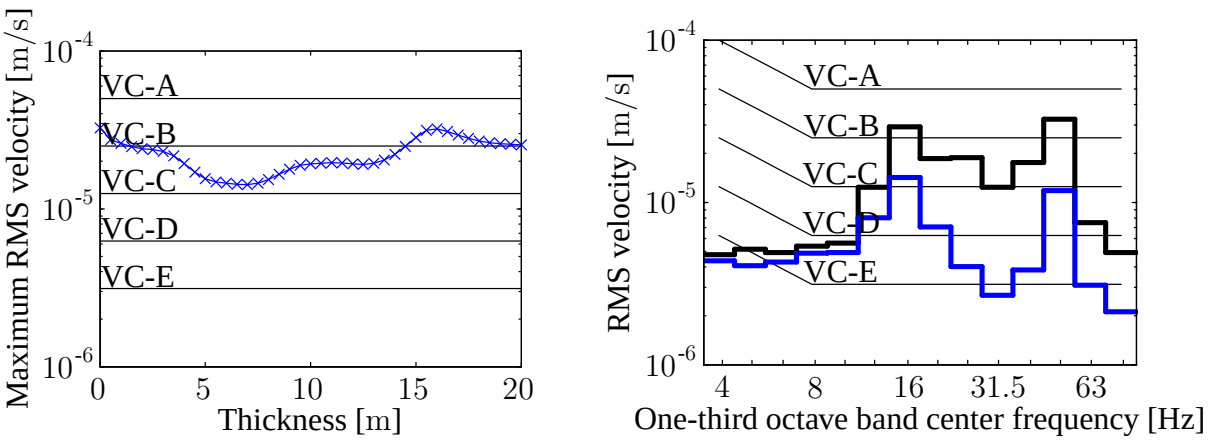

Figure 4: (a) Influence of the thickness of a rectangular wave barrier with a depth of $8\mathrm{m}$ on the maximum RMS velocity and (b) the maximum one-third octave band RMS spectra of the velocity at the receivers for the original homogeneous halfspace (black) and after the introduction of a rectangular wave barrier with a depth of $8\,\mathrm{m}$ and an optimal thickness of $7\,\mathrm{m}$ (blue).

Figure 4a shows the maximum RMS velocity for the different calculated thicknesses. It is clear that the problem is not convex, and has a global minimum around a thickness of $7\,\mathrm{m}$ in the

range considered. Figure 4b compares the one-third octave band RMS spectra of the velocity for the homogeneous halfspace and the rectangular wave barrier with the optimal thickness of $7\,\mathrm{m}$. The rectangular wave barrier provides a considerable reduction for the one-third octave bands with a center frequency higher than $12.5\,\mathrm{Hz}$, where vibration levels are reduced with a factor larger than 2 as compared to the homogeneous halfspace. However, if the VC-C criterion is aimed for, this cannot be achieved by placing a rectangular wave barrier. Moreover, the area of the cross section of the wave barrier leading to the optimal reduction is rather large, namely $8\,\mathrm{m} \times 7\,\mathrm{m} = 56\,\mathrm{m}^2$.

To overcome these limitations, the topology optimization problem in Eq. (7) is solved, where the volume is minimized and constraints are imposed on the vibration levels to meet the VC-C criterion. This is done by setting s equal to $12.5\,\mu\mathrm{m/s}$. The optimized design is shown in figure 5a. The design has a total cross sectional area equal to $6.8\,\%$ of the design domain, or $10.9\,\mathrm{m}^2$ in total.

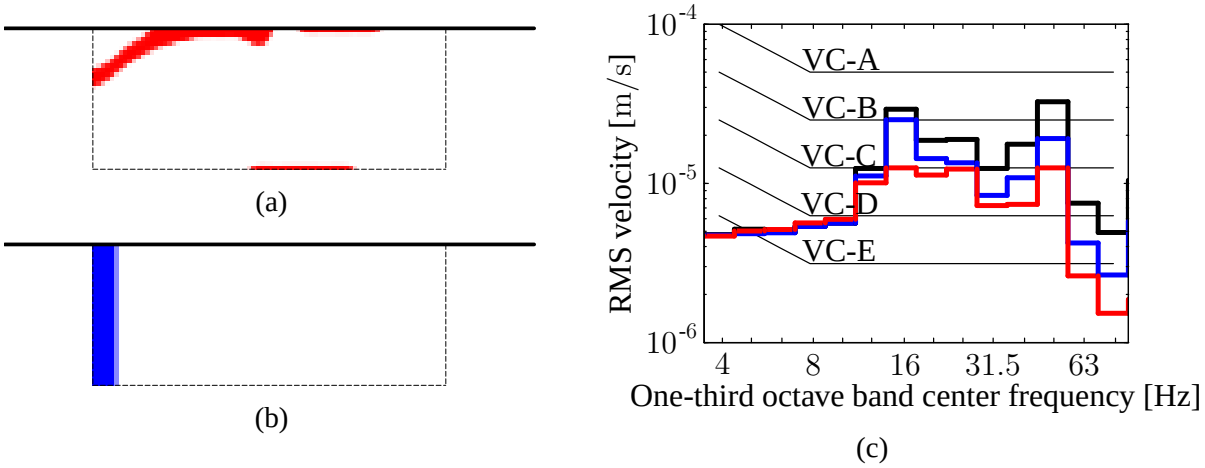

Figure 5: (a) Topology optimized design, (b) rectangular design with a depth of $8\,\mathrm{m}$ and the same volume as the optimized design, and (c) the maximum one-third octave band RMS spectra of the velocity at the receivers for the original homogeneous halfspace (black), after the introduction of the rectangular design in (b) (blue), and after the introduction of the optimal design in (a) (red).

In the optimized design of figure 5a, stiffer material is introduced in three main areas: (1) an inclined plate at the top left, (2) a horizontal plate at the surface, and (3) a horizontal plate at the bottom. The incoming waves are partly reflected by the stiffer material, partly redirected downwards into the soil by the inclined top part (1), and partly guided through the horizontal top part (2). At frequencies around $50\,\mathrm{Hz}$, a part of the waves redirected into the soil is reflected by the bottom part (3) and destructively interferes with the waves transmitted by the top part.

As the objective is to minimize the volume of the wave barrier, this optimized design is compared with a rectangular wave barrier with a depth of $8\,\mathrm{m}$ and the same volume as the optimized design. This rectangular design is shown in figure 5b. The maximum one-third octave band RMS spectra of the velocity at the receivers is compared for the two designs and for the homogeneous halfspace in figure 5c. For the homogeneous halfspace, the VC-B criterion is visibly exceeded, and only the VC-A criterion is met. Also for the rectangular design, the VC-B criterion is (slightly) exceeded in the one-third octave band with a center frequency of $16\,\mathrm{Hz}$. The optimized design, however, does not exceed the VC-C criterion, as was imposed

by the constraints. Therefore, the optimized design is not only cost efficient when compared to rectangular wave barriers, but is also more effective in reducing the vibration levels.

4 GEOMETRIC IMPERFECTIONS

The optimized design in figure 5a may be very sensitive to deviations in the geometry. The influence of geometric deviations can be modeled by varying the projection threshold η in Eq. (5), as explained in Wang et al. [12].

Figure 6 shows the influence of the projection threshold η for the optimized design in figure 5a. For low values of the projection threshold, for example $\eta = 0.25$, the projection of the filtered densities to the physical densities also includes lower values, increasing the dimensions of the stiffer material; these designs are called dilated. For high values of the projection threshold, for example $\eta = 0.75$, the projection of the filtered densities to the physical densities only includes the higher values, decreasing the dimensions of the stiffer material; these designs are called eroded.

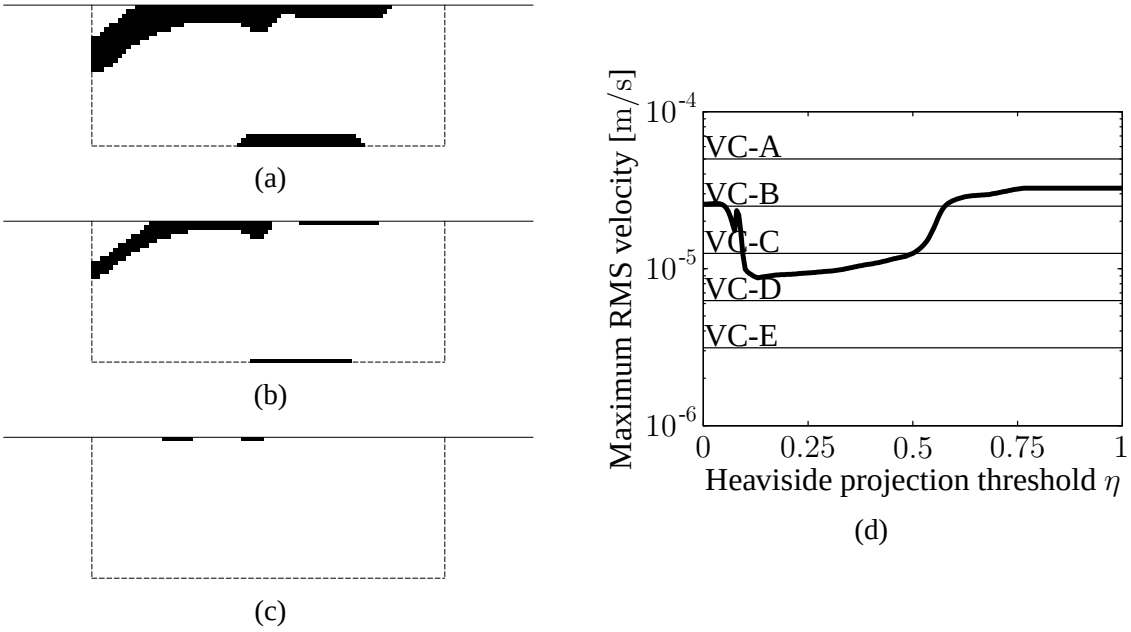

Figure 6: The (a) dilated ($\eta = 0.25$), (b) intermediate ($\eta = 0.5$), and (c) eroded ($\eta = 0.75$) version of the optimized design and (d) the influence of the projection threshold η on the maximum RMS velocity over the one-third octave bands.

Figure 6d shows that decreasing the projection threshold for example from $\eta = 0.5$ to $\eta = 0.25$ leads to a small reduction of the maximum RMS velocity over the one-third octave bands. However, increasing the projection threshold for example from $\eta = 0.5$ to $\eta = 0.75$ largely increases the maximum RMS velocity. As can be seen by comparing figures 6b and 6c, the optimized design contains only very small features which are removed when increasing the projection threshold. As a result, almost no stiffer material is left in the design domain and the performance is close to that of the homogeneous halfspace.

To obtain a design which is less sensitive to this type of geometric imperfections, a robust topology optimization approach is used. A worst case formulation is adopted where the worst performance of some (extreme) cases is optimized. Because of the smoothness of the curve

in figure 6d, good results are expected when optimizing the worst performance of only three designs with different projection thresholds ($\eta^d = 0.25$, $\eta^i = 0.5$, and $\eta^e = 0.75$). The robust optimization problem is then formulated as follows:

$$\begin{aligned} \min_{\rho_e} \quad & \sum_{e=1}^{N} v_e \bar{\rho}_e \left(\eta^i\right) \\ \text{s.t.} \quad & \hat{v}_{m,i}^{\text{RMS}} \left(\bar{\rho}_e \left(\eta^q\right)\right) \leq w_m s, \quad m = 1 \cdots N_{\text{band}} \\ & \qquad\qquad\qquad\qquad\quad i = 1 \cdots N_L \\ & \qquad\qquad\qquad\qquad\quad q = [d, i, e] \\ & 0 \leq \rho_e \leq 1, \qquad\qquad\quad e = 1 \cdots N_e \end{aligned} \tag{11}$$

where constraints are added for the dilated and eroded design.

The resulting dilated, intermediate and eroded design are shown in figure 7. Again, decreasing the projection threshold leads to a dilated design and increasing the projection threshold leads to an eroded design. However, as can be seen in figure 7d, the maximum RMS velocity does not exceed the VC-C criterion in the target interval $[0.25, 0.75]$. The volume, however, has increased as compared with the deterministic optimized design in figure 5a. The robust design has a total cross sectional area equal to $13.1\,\%$ of the design domain or $20.9\,\text{m}^2$.

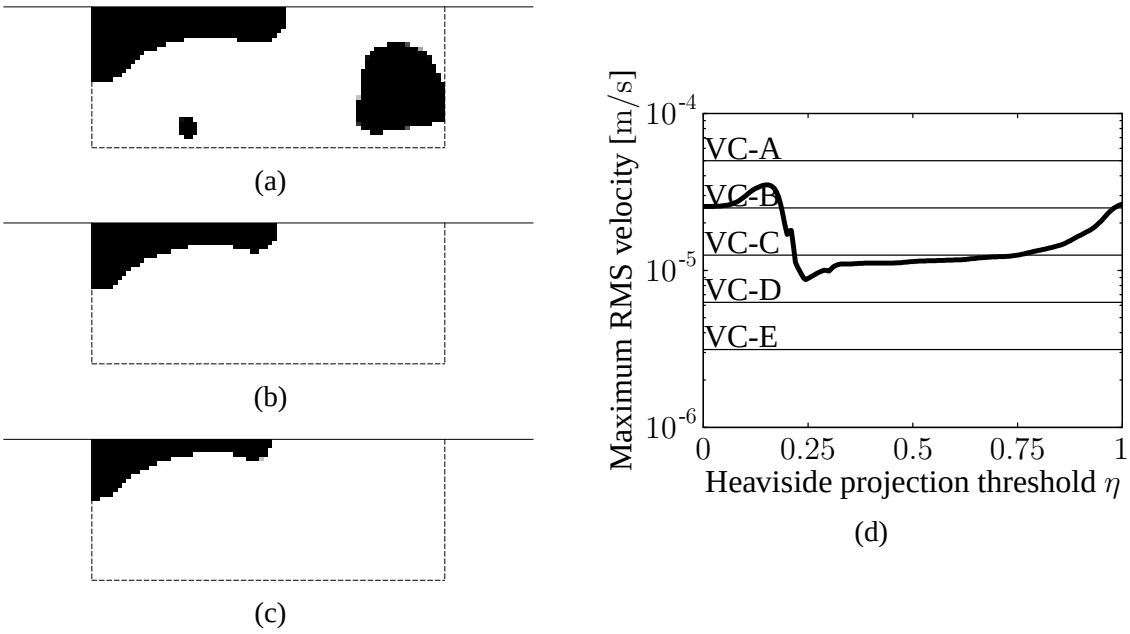

Figure 7: The (a) dilated ($\eta = 0.25$), (b) intermediate ($\eta = 0.5$), and (c) eroded ($\eta = 0.75$) version of the robust design and (d) the influence of the projection threshold η on the maximum RMS velocity over the one-third octave bands.

The performance of the intermediate robust design is compared in figure 8 with a rectangular wave barrier with a depth of $8\,\text{m}$ and the same volume as the robust optimized design. While in the original halfspace, only the VC-A criterion was met, the rectangular design just meets the VC-B criterion and the optimized design meets the VC-C criterion, as was imposed by the constraints in Eq. (11).

For practical buildability considerations, it may be desirable to simplify the design in figure 8a. Since it is robust to thickness variation, simplifying the geometry is not expected to

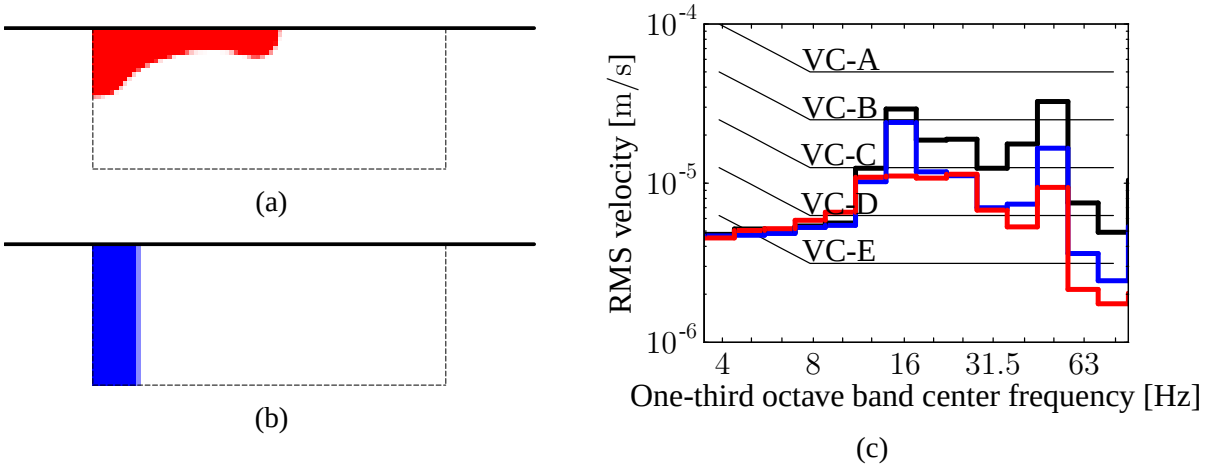

Figure 8: (a) Robust topology optimized design, (b) rectangular design with a depth of $8\,\mathrm{m}$ and the same volume as the robust design, and (c) the maximum one-third octave band RMS spectra of the velocity at the receivers for the original homogeneous halfspace (black), after the introduction of the rectangular design in (b) (blue), and after the introduction of the robust design in (a) (red).

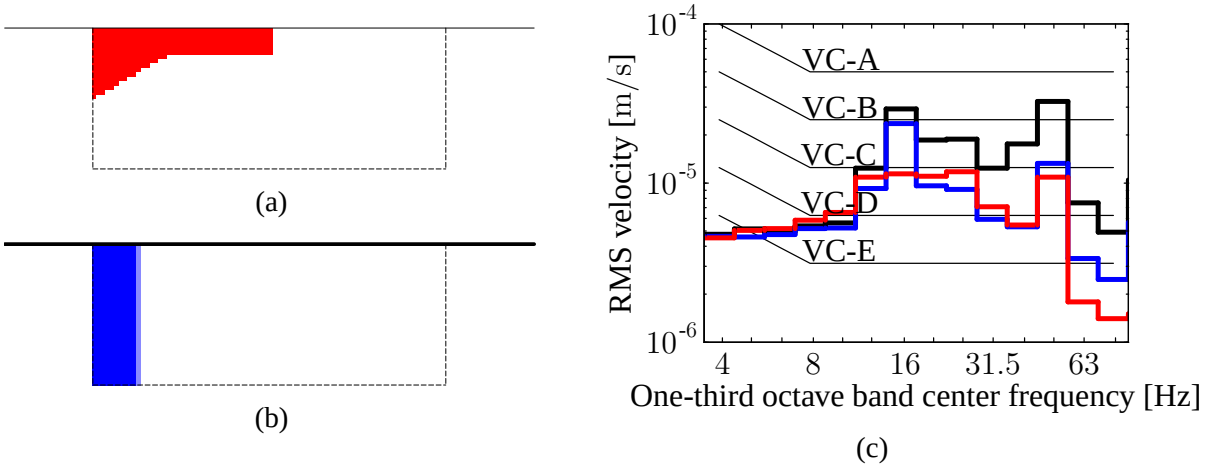

Figure 9: (a) Simplified design, (b) rectangular design with a depth of $8\,\mathrm{m}$ and the same volume as the simplified design, and (c) the maximum one-third octave band RMS spectra of the velocity at the receivers for the original homogeneous halfspace (black), after the introduction of the rectangular design in (b) (blue), and after the introduction of the simplified design in (a) (red).

significantly affect the design performance. By intuitively positioning a simplified shape with straight edges at the location where the stiffer material is concentrated in the optimized design, the design in figure 9a is obtained. This simplified design has approximately the same volume as the robust design (a cross sectional area of $20.9\,\mathrm{m}^2$) and the performance is similar, as can be seen in figure 9c. The VC-C criterion is still met.

5 CONCLUSION

In this paper, topology optimization is used to design wave barriers for the reduction of elastodynamic wave transmission. The wave barriers are located between the source, for example

a railway track, and the receivers, located in a building near the track. The volume of the wave barriers is minimized while the vibration levels have to meet stringent vibration criteria.

It is shown that rectangular wave barriers in the considered design domain are not able to meet the predefined vibration criteria. However, topology optimization leads to designs which not only meet the vibration criteria, but also need a low amount of material. The resulting design therefore outperforms the rectangular wave barrier.

Since the optimized design contains many small features, it is sensitive to geometric imperfections. A worst case approach is adopted. A larger amount of material is needed, but the resulting design is robust with respect to geometric imperfections, making it possible to simplify the topology with almost no deterioration of performance. The resulting design is buildable, cost efficient and effective in reducing vibration levels.

ACKNOWLEDGEMENTS

The first author is a doctoral fellow of the Research Foundation Flanders (FWO). The financial support is gratefully acknowledged. The authors are members of KU Leuven-BOF PFV/10/002 OPTEC-Optimization in Engineering Center.

REFERENCES

[1] G. Lombaert, G. Degrande, B. Vanhauwere, B. Vandeborght, S. François, The control of ground-borne vibrations from railway traffic by means of continuous floating slabs. *Journal of Sound and Vibration*, **297**, 946–961, 2006.

[2] L. Andersen, S.R.K. Nielsen, Reduction of ground vibration by means of barriers or soil improvement along a railway track, *Soil Dynamics and Earthquake Engineering*, **25**, 701–716, 2005.

[3] P. Coulier, S. François, G. Degrande, G. Lombaert, Subgrade stiffening next to the track as a wave impeding barrier for railway induced vibrations. *Soil Dynamics and Earthquake Engineering*, **48**, 119–131, 2013.

[4] J.P. Talbot, H.E.M. Hunt, A generic model for evaluating the performance of base-isolated buildings, *Journal of Low Frequency Noise, Vibration and Active Control*, **22**, 149–160, 2003.

[5] M.P. Bendsøe, O. Sigmund, *Topology optimization: theory, methods and applications*, Springer, Berlin, 2003.

[6] J.S. Jensen, O. Sigmund, Topology optimization of photonic crystal structures: a high-bandwidth low-loss T-junction waveguide, *Journal of the Optical Society of America B*, **22**, 1191–1198, 2005.

[7] O. Sigmund, J.S. Jensen, Systematic design of phononic band-gap materials and structures by topology optimization, *Philosophical Transactions of the Royal Society of London Series A: Mathematical, Physical and Engineering Sciences*, **361**, 1001–1019, 2003.

[8] M. Dühring, J. Jensen, O. Sigmund, Acoustic design by topology optimization, *Journal of Sound and Vibration*, **317**, 557–575, 2008.

[9] C.G. Gordon, Generic vibration criteria for vibration-sensitive equipment. *Proceedings of the SPIE Conference on Vibration Control and Metrology*, **1619**, 71–85, San Jose, California, USA, November, 1991.

[10] M. Jansen, G. Lombaert, M. Schevenels, Robust topoplogy optimization of structures with imperfect geometry based on geometric nonlinear analysis. *Computer Methods in Applied Mechanics and Engineering*, **285**, 452–467, 2015.

[11] O. Sigmund, Manufacturing tolerant topology optimization, *Acta Mechanica Sinica*, **25**, 227–239, 2009.

[12] F. Wang, B. Lazarov, O. Sigmund, On projection methods, convergence and robust formulations in topology optimization, *Structural and Multidisciplinary Optimization*, **43**, 767–784, 2011.

[13] I. Harari, U. Albocher, Studies of FE/PML for exterior problems of time-harmonic elastic waves. *Computer Methods in Applied Mechanics and Engineering*, **195**, 3854–3879, 2006.

[14] M.P. Bendsøe, Optimal shape design as a material distribution problem, *Structural optimization* **1**, 193–202, 1989.

[15] G. Rozvany, M. Zhou, T. Birker, Generalized shape optimization without homogenization, *Structural optimization* **4**, 250–252, 1992.

[16] J.K. Guest, J.H. Prévost, T. Belytschko, Achieving minimum length scale in topology optimization using nodal design variables and projection functions. *International Journal for Numerical Methods in Engineering*, **61**, 238–254, 2004.

[17] K. Svanberg, The method of moving asymptotes – a new method for structural optimization. *International Journal for Numerical Methods in Engineering*, **24**, 359–373, 1987.